Carbohydrate Polymers 77 (2009) 280–287

Contents lists available at ScienceDirect

Carbohydrate Polymers

journal homepage: www.elsevier.com/locate/carbpol

Bacterial and plant cellulose modification using ultrasound irradiation

Shen-Siung Wong [a], Stefan Kasapis [b,*], Yanfang Mabelyn Tan [a]

[a] Food Science & Technology Programme, Department of Chemistry, National University of Singapore, Block S3, Level 6, Science Drive 4, 117543, Singapore
[b] School of Applied Sciences, RMIT University, Bundoora West Campus, Melbourne, Vic 3083, Australia

ARTICLE INFO

Article history:
Received 14 August 2008
Received in revised form 8 November 2008
Accepted 23 December 2008
Available online 14 January 2009

Keywords:
Bacterial cellulose
Ultrasonication
SEC
X-ray
TGA
FTIR
TEM

ABSTRACT

This study indicates that controlled depolymerization of plant (PC) and bacterial (BC) celluloses can be achieved by employing suitable ultrasonication settings. Size exclusion chromatography results indicate that reduction in the molecular weight of the two polymers was accompanied by a parallel drop in the polydispersity index of PC and an unexpected increase in the said index of BC. X-ray diffraction patterns of the fractionated materials were found to be Cellulose II crystals whereas experimentation on microcrystalline cellulose unveiled the Cellulose I conformation. The crystallinity index revealed no obvious changes in PC as a function of the time of sonication whereas a major increase in the crystalline component was encountered for BC. Furthermore, thermal degradation using TGA and FTIR spectra suggest that the processes of dissolution and regeneration in cuprammonium hydroxide of PC and BC followed by ultrasonication do not affect the chemical fingerprints *via* oxidative reactions of the cellulosic materials.

1. Introduction

Cellulose is the principle cell wall component of higher plants and hence the most abundant biopolymer on earth. It is a high molecular weight, linear, water-insoluble homoglycan of repeating β-D-Glucopyranosyl units joined by β-D-(1 → 4) glycosidic linkages (Klemm, Heublein, Fink, & Bohn, 2005). For many centuries, plant-derived cellulose has been utilised extensively by the paper and textile industries leading to a significant demand on wood biomass. Recently, the pharmaceutical, cosmetic and food industries have considered utilisation of plant cellulose but its high molecular weight and water-insoluble character has somehow restricted direct incorporation in various applications. To address this, a depolymerised form of cellulose known as microcrystalline cellulose (MCC) and various water or nonpolar-solvent soluble derivatives of the material have been developed as structuring or suspending aids (El-Sakhawy & Hassan, 2007).

Owing to its high crystallinity, unique mechanical properties and renewable nature, the utilization of crystalline cellulose and its derivatives as a reinforcing filler in polymer composites has gained wide attention. Commonly, MCC is produced by acid hydrolysis of α-cellulose (Klemm et al., 2005). The process cleaves the polymer backbone preferably at the less crystalline regions, leaving fragments with lower molecular weight and high crystallinity. Obtaining crystalline cellulose via acid hydrolysis has been extensively studied and it is a well established industrial process (Roman & Winter, 2004; Wang, Ding, & Cheng, 2007). Nevertheless, energy saving environmentally friendly methods, and yet capable of retaining desired functionality, in particular thermostability and crystallinity in the end product, are sought after alternatives to chemical modification.

Ultrasound irradiation (or sonication) affords a promising alternative to conventional hydrolysis methods. Mason and Lorimer (2002) define ultrasound as sound having a frequency higher than the human hearing range, i.e. >20 kHz. The ability of ultrasound in degrading polymeric sequences has been well documented, particularly in synthetic materials dissolved in various solvents. In the case of biopolymers, studies have dealt with chitosan (Baxter, Zivanovic, & Weiss, 2005; Chen, Chang, & Shyur, 1997; Liu, Bao, Du, Zhou, & Kennedy, 2006), cellulose derivatives (e.g., carboxymethylcellulose (Gronroos, Pirkonen, & Ruppert, 2004), cellulose nitrate (Marx-Figini, 1997)) and other water soluble polysaccharides such as guar gum (Tayal & Khan, 2000), dextran (Cote & Willet, 1999; Lorimer, Mason, Cuthbert, & Brookfield, 1995; Portenlanger & Heusinger, 1997), agarose and carrageenans (Lii, Chen, Yeh, & Lai, 1999).

To the best of our knowledge, scientific works on the effect of ultrasound treatment on the structural properties of water-insoluble plant cellulose (PC) and bacterial cellulose (BC) are rather scarce. Marx-Figini (1997) has conducted a study on ultrasound degradation of cellulose nitrate in ethyl acetate. As for the sulfate groups present in carrageenans (Lii et al., 1999), the presence of nitrate groups in the cellulose backbone imparts charge density and

* Corresponding author. Tel.: +61 3 9925 7144; fax: +61 3 9925 7110.
E-mail address: stefan.kasapis@rmit.edu.au (S. Kasapis).

0144-8617/$ - see front matter © 2009 Elsevier Ltd. All rights reserved.
doi:10.1016/j.carbpol.2008.12.038

steric hindrance, which affect the degradation profile. Moreover, the ester linkage joining the nitrate group with the cellulose backbone is subject to hydrolysis, a similar phenomenon to the deacetylation of chitin upon ultrasonication (Liu et al., 2006).

In the present study, the degradation patterns of underivatized PC and BC are examined in an effort to control the molecular weight distribution of these materials whose structural properties will then be characterised using an armory of complementary physicochemical techniques.

2. Experimental

2.1. Materials

Plant cellulose was a fibrous medium from cotton lint, and with powdered MCC, was purchased from Sigma–Aldrich, Munich, Germany. Bacterial cellulose was produced as follows: Gluconacetobacter xylinus (ATCC® 700178, Manassas, USA) stored previously in a frozen MicrobankTM (Pro-Lab Diagnostics, Richmond Hill, Canada) was used. Yeast glucose carbonate (YGC) medium consisting of 5% (w/v) D-glucose, 0.5% (w/v) yeast extract and 1.25% (w/v) calcium carbonate was used for the inoculum preparation and BC production. All media and apparatus were autoclaved at 121 °C and 1.02 atm for 15 min. A single bead was drawn from a frozen MicrobankTM, promptly cultured on a YGC agar plate (with 1.5% (w/v) bacteriological agar) and incubated at 26 °C for 72 h.

Separate colonies were aseptically transferred to 500 ml of a seed fermentation medium followed by static incubation at 26 °C for 72 h. Thirty six milliliters of this medium were inoculated aseptically into an aluminium tray (260 mm width × 345 mm length × 55 mm height) containing 1164 ml YGC medium. The tray was covered with aluminium foil and incubated statically at 26 °C for 12 days. Bacterial cellulose pellicle formed at the liquid–air interface of the fermentation medium was removed, rinsed thoroughly with deionised water and boiled in deionised water for 15 min. Following this, the pellicle was immersed four times in a solution of 0.1 N NaOH held each time at 80 °C for 2 h, rinsed, boiled (15 min), soaked overnight and washed repeatedly with deionised water until washings became neutral to methyl red, and lyophilized.

Purified bacterial cellulose and plant cellulose were then ultrasonicated. That required the following preparation of cuprammonium hydroxide solution (CUAM) (method of Kamide and Nishiyama (2001), with some modifications): Sixty grams of CuSO4.5H2O were dissolved into 1 L of hot water (90 °C) followed by addition of 23 ml of 25% (w/v) ammonia solution (50 °C) to form the basic copper sulfate precipitate. That was washed with hot deionised water and the supernatant was discarded. Two hundred millilitres of 20% (w/v) NaOH were added to form the blue copper hydroxide precipitate, which was washed twice with cold deionised water. The precipitate was vacuum filtered (Whatman No. 1) and the retentate was further washed with cold deionised water until the filtrate was free from sulfate ions (tested with 1 M $CaCl_2$). Copper hydroxide was oven dried overnight at 50 °C, transferred into a screw cap bottle in the presence of 1400 ml of 20% (w/v) ammonia solution and the mixture was shaken vigorously. The precipitate of excessive copper hydroxide was removed by filtering under vacuum and the dark blue filtrate was the CUAM solution used.

Homogeneous solutions of 0.125% (w/v) PC and BC were made in CUAM and left at ambient temperature for 2 h. Ultrasonication (Elmasonic S 60H, ELMA, Singen, Germany) of both materials was carried out at a frequency of 37 kHz and effective ultrasonic power of 150 W for the time periods of 5, 10, 15 and 30 min. PC and BC were recovered from solution by addition of 1 M H_2SO_4, which led to the formation of a white precipitate. That was filtered under vacuum, washed with deionised water until the filtrate became neutral to methyl red, dialysed and lyophilized to produce neutral cellulosic materials.

2.2. Size exclusion chromatography (SEC)

The method of Dupont (2003) with some modifications was used to prepare PC, BC and MCC for size exclusion chromatography: Deionised-water preparations of cellulose (0.6% w/v) were subjected to consecutive exchanges/activation steps of methanol (two – 1 h each) and dry *N*,*N*-dimethyl acetamide (DMAc) (two – 1 h and overnight) with constant stirring. Following this, activation liquids were discarded by filtering under vacuum, and DMAc/8% LiCl was added to form dissolved cellulose solutions of 1.2% (w/v). Dilution with dry DMAc gave a final concentration of 0.24% (w/v) with respect to the cellulosic sample and 1.6% (w/v) with respect to LiCl.

The SEC system with manual injector included a Waters 515 HPLC Pump and a Waters 410 refractive index (RI) detector (Waters Corporation, Milford, USA). Prior to injection, samples and mobile phase (DMAc/0.5% LiCl) were filtered through a PTFE membrane filter. The injection volume was 250 μl, separation was performed on a series of three Phenogel mixed bed columns (300 × 7.8 mm; particle size 10 μm) at 65 °C, and at the flow rate of 0.8 ml/min. Each sample run lasted for 50 min. Nine pullulan standards of narrow polydispersity, i.e., 788, 404, 212, 112, 47.3, 22.8, 11.8, 5.9 and 0.67 kDa (Polymer Laboratories, Church Stretton, UK) were used to calibrate the columns. The linear coefficient of determination (r^2) between the weight average molecular weight ($\overline{M}w$) of the standards and elution time was 0.999. Data acquisition and processing were done by using Waters Empower data software Version 5.00.

2.3. X-ray powder diffraction studies (XRPD)

X-ray powder diffraction patterns were obtained using a SIEMENS D5005 X-ray Diffractometer (Bruker AXS, Karlsruhe, Germany) equipped with Cu-K_α (1.54 Å) radiation. An accelerating voltage and current of 40 kV and 40 mA, respectively, in combination with a scan rate of 0.8 °C/min were employed. The diffractograms were recorded in a 2θ range between 5° and 45°, and subsequently analyzed using the Bruker Advanced X-ray Solutions software, DIFFRACplus Evaluation (Eva), version 10.0 revision 1.

Diffraction profiles of the samples were fitted with a Gaussian function to resolve into separate diffraction peaks and subsequent integration was performed on each peak. PC and BC spectra were resolved into three peaks corresponding to 101, $10\bar{1}$ and 002 crystal planes but the MCC spectrum exhibited an additional 040 crystal plane. The crystallinity index (CrI) of samples was determined following the method reported by Wang et al. (2007) with slight modifications:

$$\mathrm{CrI} = \frac{A_{\mathrm{Crystal}}}{A_{\mathrm{Total}}} \times 100$$

where, A_{Crystal} is the sum of the areas under the crystalline diffraction peaks and A_{Total} represents the total area under the diffraction curve between 2θ of 5° and 45°.

2.4. Thermogravimetric analysis (TGA)

This was carried out to determine the thermal stability of our materials by employing a thermogravimetric analyzer, SDT 2960 (TA Instruments, New Castle, DE). Samples were heated from ambient temperature to 600 °C in a nitrogen current of 100 ml/min at a heating rate of 10 °C/min. Thermogravimetric (TG) curves and

derivative TG (DTG) curves were analyzed with the aid of the TA Instruments Universal Analysis Software (Version 3.9A) in an effort to determine the peak onset temperature and peak maximum temperature.

2.5. Fourier transformed infrared (FTIR) spectroscopic analysis

Prior to analysis by FTIR spectroscopy, samples and potassium bromide (KBr) were dried in an oven overnight at 50 °C. FTIR data were obtained with a Spectrum One FTIR Spectrophotometer (Perkin-Elmer, Norwalk, CT) by employing KBr as the sample holder. A single background scan was performed followed by a hundred sample scans at a resolution of 4.00 cm^{-1} in order to produce the final spectrum. Recording was within the range of 4000–400cm^{-1} and data acquisition was facilitated by the Spectrum v5.0.1 Software of Perkin-Elmer.

2.6. Transmission electron microscopy (TEM)

Disintegrated cellulose crystals, which were produced by the combined CUAM/ultrasonication treatment, were suspended in deionized water. This was followed by deposition of a few droplets of the suspension onto a Formvar coated copper grid with a mesh size of 200. Copper grids with cellulose crystals were loaded into a sample chamber following air drying. Electron micrographs of tested materials were recorded by a Philip CM10 transmission electron microscope (Philip, Eindhoven, Netherlands) operated at 100 kV. Micrographs were taken using Kodak Electron Microscopy film 4489 (Eastman Kodak Company, New York, USA) and converted into a digital form with a conventional digital photo scanner.

3. Results and discussion

3.1. Effect of ultrasound sonication on the weight average molecular weight and polydispersity index

Fig. 1 reproduces the SEC elution patterns of ultrasonicated bacterial and plant cellulose in DMAc/0.5% LiCl. The treatment has affected the retention time, with the ultrasonicated samples having longer retention times compared to that of the control (BC-0 and PC-0). Slowly eluting materials possess small molecular weight and Fig. 2 summarizes the effect of ultrasonication time on the degradation patters (weight average molecular weight) of BC and PC.

The decrease in $\overline{M}w$ is attributable to scission of the β-D-(1 → 4) glycosidic linkages. Mason and Lorimer (2002) dealt in detail with the hydrodynamic force and shear stress generated from the cavitation of bubbles, which are the outcome of the ultrasound treatment of polymeric solutions. The treatment amounts to alternating compression and rarefaction processes that make bubbles to rapidly form and collapse within the solution. Tested materials have been subjected to a relatively short period of treatment (maximum of 0.5 h). Therefore, further reduction in molecular weight is anticipated upon prolonged periods of ultrasonication. Sonication of chitosan (Liu et al., 2006) and cellulose nitrate (Marx-Figini, 1997) solutions has been reported for 100 h and 1.5 h, respectively, and within this time period of experimentation, the decrease in molecular weight approaches asymptotically a "level-off degree of polymerization".

Another issue to consider is the use of cuprammonium hydroxide as the solvent of underivatized cellulose. CUAM can dissolve the polymer without having to perform pre-dissolution activation steps. Moreover, sonicated materials can be recovered readily from the aqueous solution for further characterizations, as compared to organic solvents (e.g. DMAc/LiCl) which has been used by Striegel (2007). However, ammonia in CUAM is volatile and according to Price et al. (Price, West, & Smith, 1994), ultrasound degradation is less efficient in such a highly volatile solvent. This observation may bear an effect on the ultrasonication profile of plant and bacterial cellulose. Nevertheless, degradation has been observed in a relatively short period of time (within 0.5 h) in the current study, unlike the report by Striegel (2007) where degradation became

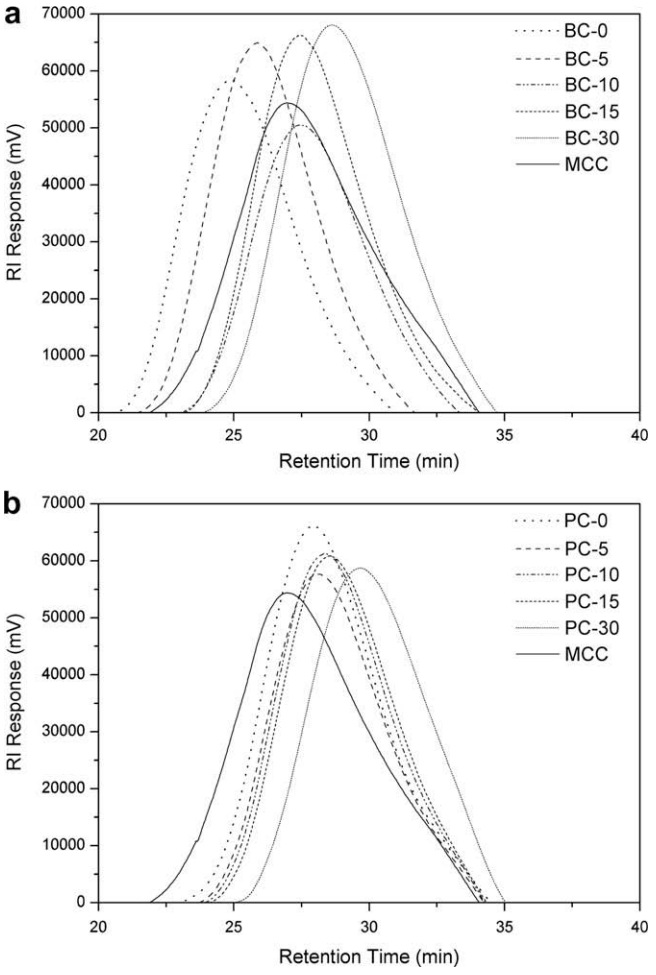

Fig. 1. SEC elution patterns of ultrasonicated (a) BC and (b) PC in DMAc/0.5% LiCl.

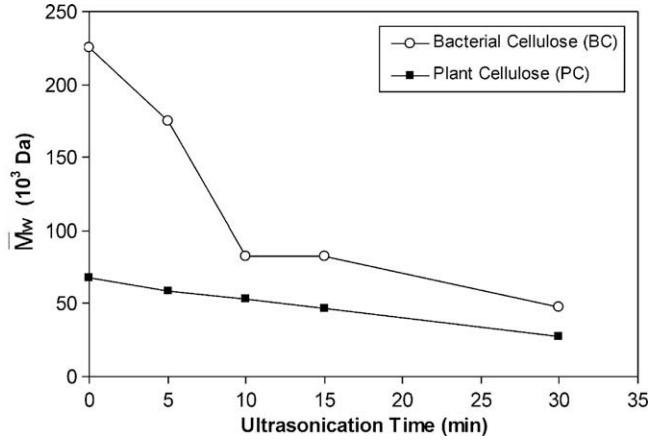

Fig. 2. Weight-average molecular weight variation of plant and bacterial cellulose as a function of ultrasonication time.

pronounced in 2 h using DMAc/LiCl. This further confirms that CUAM is a potent solvent for the ultrasound degradation of cellulose.

The average molecular weight of bacterial cellulose shows a drastic fall at the beginning of ultrasonication (≈64% reduction in the first 10 min), which is followed by a gradual decrement at longer times. In comparison, $\overline{M}w$ reduction of PC followed a steady declining trend throughout the experiment period of observation, and the reduction was relatively limited (≈21% within 10 min of ultrasonication). It appears that as for chitosan (Liu et al., 2006), high molecular weight bacterial cellulose is amenable to ultrasonicated depolymerisation. The increased density of such molecular weight fractions in the material at the beginning of ultrasonication warrantees high degradation rates at the first stage of experimentation. In addition, Gronroos et al. (2004) postulated that below a certain limit of molecular weight, the short polymer chains might follow flexibly the ultrasonic vibration thus escaping covalent-bond cleavage.

The second part of this section examines the polydispersity index (PI), which is an indication of the segmental size distribution of a particular polymer defined as the ratio of weight to number ($\overline{M}n$) average molecular weight. Fig. 3 depicts the effect of increasing ultrasonication time on the PI of plant and bacterial cellulose. The reduction in the polydispersity index of PC is consistent with the idea that prolonged sonication yields chain segments that can not be further degraded, an outcome which tends to create homogeneous systems with a relatively narrow molecular weight distribution (Gronroos et al., 2004). This is in agreement with the work on chitosan (Chen et al., 1997), where degradation stops and low values of the polydispersity index are obtained once a limiting molecular weight for this system is reached at 1.8×105 Da.

In contrast to the results of the preceding paragraph, the PI of bacterial cellulose exhibited a noticeable increase during the course of experimentation (Fig. 3). The rapid reduction in $\overline{M}n$ as compared to that of $\overline{M}w$ is rather unexpected for ultrasonication treatments. It is known in enzymatic (Klemanleyer, Gilkes, Miller, & Kirk, 1994; Tayal & Khan, 2000), and acid hydrolysis (Shibazaki, Kuga, Onabe, & Brown, 1995) of polysaccharides, which is attributed to a random scission process. Plant and bacterial cellulose are chemically identical but the supramolecular structure, i.e., the morphological characteristics of the cellulose microfibrils are quite distinct (Klemm et al., 2005). In addition, the susceptibility of polysaccharides to ultrasonic degradation is subject to their conformational state in solution (Lii et al., 1999). Thus, "single" helices of carrageenan in solution offer greater resistance to degradation than their random-coil counterparts (Lii et al., 1999). Bacterial cellulose in this work was properly dissolved in preparation for ultrasonication and, therefore, the conformational characteristics of the material in CUAM may prove to be of critical importance.

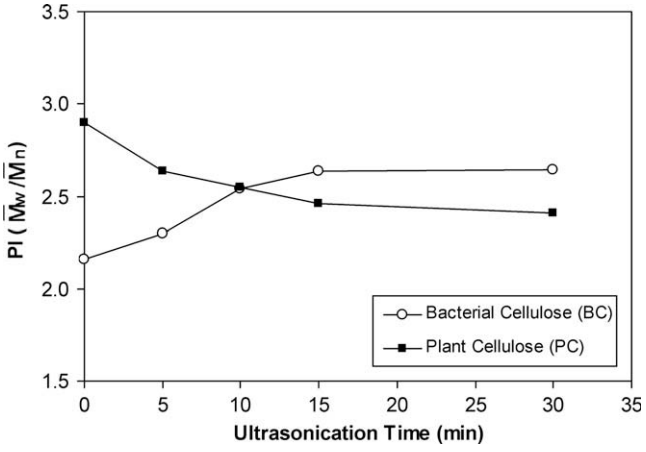

Fig. 3. Polydispersity-index variation of plant and bacterial cellulose as a function of time of ultrasonication.

The molecular dimensions of plant/bacterial cellulose were compared to those of a sample of microcrystalline cellulose. MCC was found to possess a weight average molecular weight of ≈99.30 kDa with a polydispersity index of ≈3.60. This is distinct from the $\overline{M}w$ of PC and should be attributed to natural or processing variations of the material. Furthermore, MCC samples obtained from different sources of cellulose are expected to exhibit dissimilar physicochemical properties (such as molecular weight) even though similar acid hydrolysis conditions are employed. Interestingly, bacterial cellulose ultrasonicated between 10 and 15 min possesses similar $\overline{M}w$ to that of MCC. The broad agreement in the molecular dimensions of BC and MCC is encouraging as a first step for considering industrial applications for the molecular fractions of bacterial cellulose.

3.2. X-ray diffraction profile and crystallinity index (CrI)

Fig. 4a illustrates the X-ray diffraction patterns of bacterial cellulose sonicated at different time periods (0, 5, 10, 15, and 30 min) at ambient temperature. Three major diffraction peaks at 2θ equal to 12.0°, 20.0° and 21.8° were resolved from the deconvolution process and these become sharper with increasing time of sonication. X-ray studies of plant cellulose reveal similar diffraction patterns for each time period of observation with some noticeable differences in peak intensity (Fig. 4b). According to the literature, this X-ray diffraction profile is compatible with what is known as the "Cellulose II crystal" (Oh et al., 2005; Shibazaki et al., 1995). Conversely, MCC shows four diffraction peaks, which are ascribed to the crystallographic planes of 101, $10\bar{1}$, 002 and 040 at 2θ equal to 14.8°, 16.4°, 22.5° and 34.4°, respectively. This is known in the literature as the conformation of the "Cellulose I crystal" (Cao & Tan, 2004).

The mutant strain of Gluconacetobacter xylinus, ATCC® 23769, has been reported to produce the so called "native band cellulose", which exists as the Cellulose II allomorph (Shibazaki et al., 1995) but, normally, natural occurring cellulose (BC and PC) exists in the thermodynamically less stable Cellulose I allomorph (Yamamoto, Horii, & Hirai, 2006). Besides ultrasonication, cellulosic materials of the present work have been subjected to dissolution and subsequent regeneration, a course of action that should transform Cellulose I to the more stable Cellulose II structure. Thus the mercerization process, which involves dissolution/swelling of cellulose in aqueous NaOH followed by regeneration/neutralization with HCl, is known to transform Cellulose I into Cellulose II (Shibazaki, Kuga, & Okano, 1997). There is scant literature addressing the effect of CUAM but Miyamoto and co-workers (Miyamoto, Matsuoka, Matsui, Saito, & Okajima, 1996) have shown that plant cellulose recovered from the solvent projects an X-ray diffraction profile with two major peaks at 2θ equal to 20.0° and 21.9°, which is associated with the Cellulose II allomorph.

For the crystalline component of cellulosic materials, the first observation is that the crystallinity index of microcrystalline cellulose is the highest (87.6%; Table 1). Furthermore, the CrI of non-sonicated BC (55.6%) is well below that of PC (72.2%), with the latter being comparable to data obtained by Miyamoto et al. (1996). The crystalline fraction of plant cellulose remains unaffected by the duration of ultrasonication, an outcome which is attributed to the rapid formation of the stable Cellulose II allomorph within 3 min of mercerization (Shibazaki et al., 1997). It appears, however, that ultrasonication is capable of increasing considerably the level of crystallinity of bacterial cellulose to 75.4% within 30 min of treatment. It is known that increasing exposure of bacterial cellu-

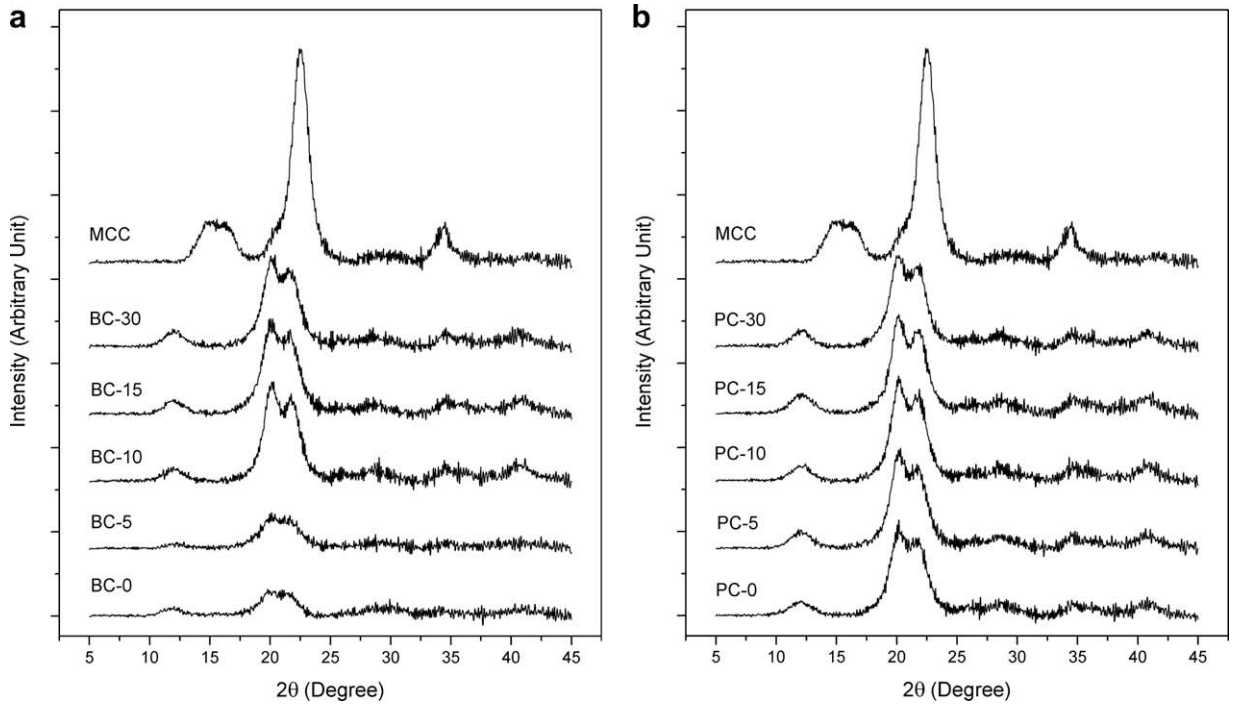

Fig. 4. X-ray diffraction pattern of (a) bacterial cellulose and (b) plant cellulose sonicated at different times, and compared to those of MCC.

Table 1
Crystallinity index (CrI), peak onset temperature, T_e (°C) and peak maximum temperature, T_{max} (°C) of bacterial cellulose (BC) and plant cellulose (PC) ultrasonicated at different times.

Sample	Ultrasonication time (min)	Crystallinity index (%)	Peak onset temperature, T_e (°C)	Peak maximum temperature, T_{max} (°C)
MCC	–	87.6	312.0	337.1
BC-0	0	55.6	301.1	324.7
BC-5	5	63.6	314.9	332.2
BC-10	10	71.0	311.1	333.8
BC-15	15	73.2	308.9	333.7
BC-30	30	75.4	313.1	333.4
PC-0	0	72.2	302.1	329.8
PC-5	5	72.3	307.6	330.9
PC-10	10	71.6	308.1	328.9
PC-15	15	71.2	305.6	326.3
PC-30	30	71.4	311.3	334.0

lose to aqueous NaOH raises the crystalline content of the recovered material (Shibazaki et al., 1997). Exposure of BC to copious amounts of OH- from CUAM used in the present study should contribute towards the increment of CrI. Nevertheless, all materials were exposed roughly to the same dissolution time in CUAM hence it is argued that the variable time of ultrasonication also plays a significant role in promoting crystallinity in bacterial cellulose by reducing its molecular weight distribution.

3.3. Thermal degradation of cellulosic materials

To evaluate the thermostability of ultrasonicated samples, thermogravimetric analysis (TGA) was performed on bacterial and plant cellulose, and results were compared to those of the commercial microcrystalline cellulose. TG and derivative TG (DTG) curves of BC and PC are depicted in Fig. 5(a–d), respectively. Experimental profiles in Fig. 5a and c exhibit sharp steps of weight loss indicative of degradation processes in the macromolecules. DTG curves of the experimental data show two peaks throughout the pyrolytic scan (Fig. 5b and d).

The low temperature event centers at about 50 °C and it is a relatively small peak that corresponds to the evaporation of water molecules adsorbed to the polymeric sequences. The dominant peak between 300 and 350 °C was caused by the weight loss arose from concurrent cellulose degradation processes. These include depolymerization, further dehydration, degradation of the glucopyranosyl units and subsequent oxidation leaving behind charred residues (Roman & Winter, 2004). The degradation patterns in terms of shape and temperature band appear to be quite similar for all materials. Within this cluster of traces, MCC and BC-0 exhibit the highest and lowest thermal stability, respectively. Data have been tabulated to afford unambiguous comparisons of the peak onset temperatures (T_e) and peak maximum temperatures (T_{max}) of materials at different stages of ultrasonication. Wang et al. (2007) suggested that the more ordered the cellulose the higher the energetic requirements for polymeric degradation. Table 1 indicates such a trend for the extreme cases of BC-0 and MCC (lowest and highest CrI) but, in general, the T_e and T_{max} values of all materials are comparable.

Normally, chemical alteration of the polymer affects the degradation profile which spreads over a wide temperature range causing noticeable broadening of the DTG peak. Thus, Roman and Winter (2004) reported that the presence of sulfate groups in cellulose accelerates the onset and broadens the temperature fingerprint of degradation. Furthermore, the presence of an oxidized moiety in cellulose will yield multimodal steps of thermal decomposition, an outcome which is confirmed by the present of additional peaks in the DTG figure (Varma & Chavan, 1995). In the absence of such "anomalies" and since the thermal degradation is largely insensitive to the changing component of crystallinity, it can be argued that chemical oxidation has not taken place during dissolution, regeneration or ultrasonication of the cellulosic materials investigated presently.

3.4. Fourier transform infrared analysis (FTIR)

Fig. 6a and b depict the FTIR spectra of bacterial and plant cellulose at distinct durations of ultrasonication, which are then com-

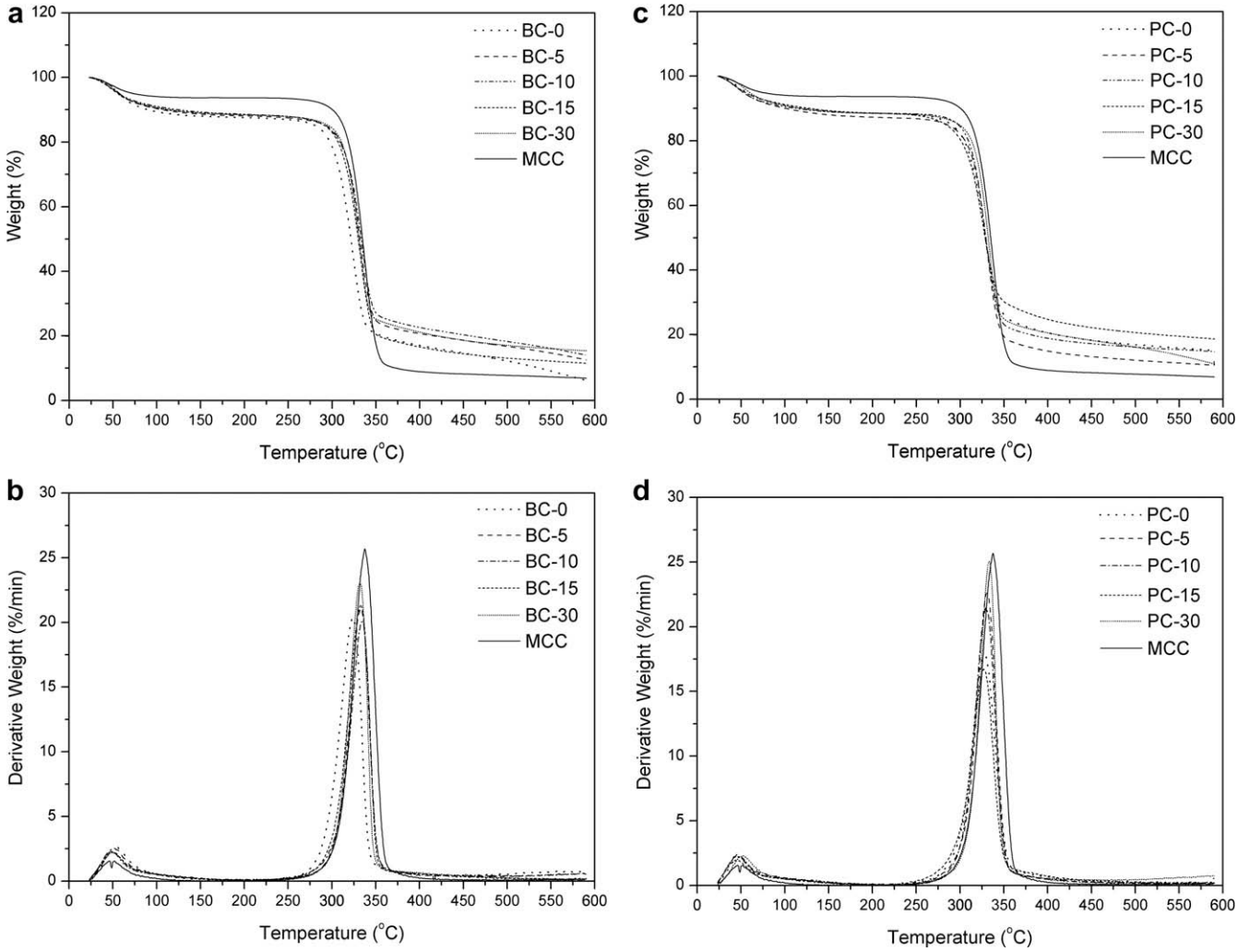

Fig. 5. TG and DTG curves of ultrasonicated samples of bacterial cellulose (a and b) and plant cellulose (c and d).

pared with those of microcrystalline cellulose. FTIR spectroscopy is a useful tool in elucidating the functional groups of organic macromolecules, as well as understanding the bonding interactions of these functional groups. Thus it is utilised to provide key information on the nature of molecular forces that dominate the transformation of the cellulose crystal during the present treatment. The detailed designation of each wavelength band to a specific functional group has been reported previously by others (Carrillo, Colom, Suñol, & Saurina, 2004; Oh et al., 2005).

Visual examination of the FTIR spectra of BC and PC with or without ultrasonication shows a broad adsorption peak that bottoms out at about 3447 cm^{-1}. This is attributed to the stretching of hydroxyl groups involved in intramolecular hydrogen bonding of the Cellulose II crystal. MCC, on the other hand, shows the –OH stretching peak at about 3350 cm^{-1} hence indicating the conformation of the Cellulose I crystal. Both observations confirm the argument of the X-ray diffraction study (Section 3.2) that acid hydrolysis of cellulose retains in MCC the Cellulose I allomorph whereas dissolution and regeneration convert the material into the thermodynamically stable Cellulose II crystal.

The lack of an absorption band in the range of 1740–1745 cm^{-1} for all materials argues for the absence of carbonyl groups (C=O), which are usually present in oxidized cellulose either as part of the carboxyl (COO^-) or aldehyde group (HC=O) (Kim, Kuga, Wada, Okano, & Kondo, 2000; Son, Youk, & Park, 2004). A peak at 1740 cm^{-1} can be detected in oxidized cellulose with a degree of oxidation as low as 0.12 (Kim et al., 2000). Furthermore, the presence of a pattern of peaks between 894 and 897 cm^{-1} for BC, PC and MCC reveals the stretching of C—O—C bonds at β-glycosidic linkages (Oh et al., 2005). Results discussed in this paragraph are in agreement with the observations from the thermogravimetric study (Section 3.3) that material preparation in CUAM and subsequent ultrasonication did not cause oxidative reactions on the chain segments of cellulose. It should be noted that Cao and Tan (2004) using the enzyme cellulase to depolymerise plant cellulose reported FTIR spectra in accordance with the original untreated sample.

3.5. Transmission electron microscopy (TEM)

There is scant information in the literature on the microscopic morphology of ultrasonicated cellulosic materials especially those that have been dissolved and subsequently regenerated. In this case, the resulting particle characteristics are expected to be influenced by both ultrasonication and regeneration. Fig. 7 depicts the TEM micrographs of selected ultrasonicated BC and PC samples, and microcrystalline cellulose. These appear to be discrete and isolated particles, and MCC possesses the most regular and ordered structures with defined edges, an outcome which should be attributed to the high level of crystallinity (87.6% in Table 1) of this

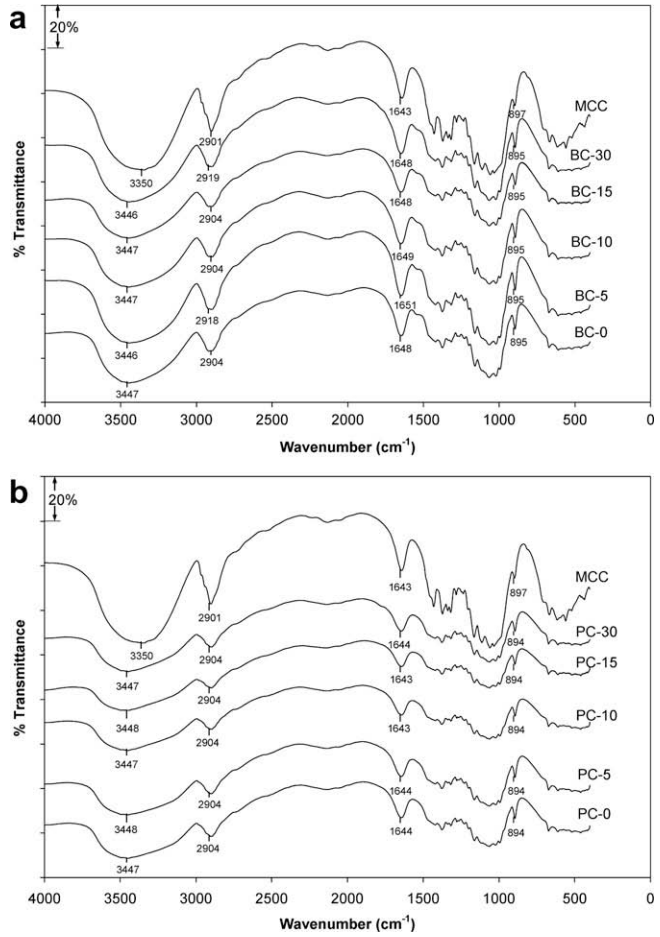

Fig. 6. FTIR spectra of (a) bacterial cellulose and (b) plant cellulose ultrasonicated at different times, and compared to those of MCC.

material. Clearly the current process of ultrasound sonication is capable of yielding small-size particles within 30 min of treatment in accordance with the variation in molecular weight of plant and bacterial cellulose in Fig. 2. During the regeneration process, addition of sulfuric acid neutralises the hydroxyl ion and forms copper sulfate in CUAM thus making dissolution of cellulose molecules unfavorable. It seems that the short period (about 60 s) of the regeneration process in the present investigation results in a spontaneous aggregation of the microfibrils of bacterial and plant cellulose, which possess relatively irregular particle shapes. Furthermore, the abundant positive charge of the solution contributed by the excessive levels of sulfuric acid added during regeneration should further enhance the stability of the small-size (about 1 μm) particles via electrostatic repulsion.

4. Conclusions

The present work has achieved an efficient depolymerisation process of cellulose without having to prior derivatize the biopolymer. Findings concluded that ultrasonication of cellulose in CUAM will not induce undesirable chemical modifications (e.g., oxidative reactions) and the shorter polymeric segments of the sonicated product remain β-1,4-D-glucan. It is of interest to observe that fractionated plant and bacterial celluloses are of the type II crystal whereas microcrystalline cellulose possesses the crystal I conformation. Furthermore, it is argued that long ultrasonication times yield a high crystallinity index for the ultrasonicated BC, an outcome that merits further investigation. Highly crystalline cellulose

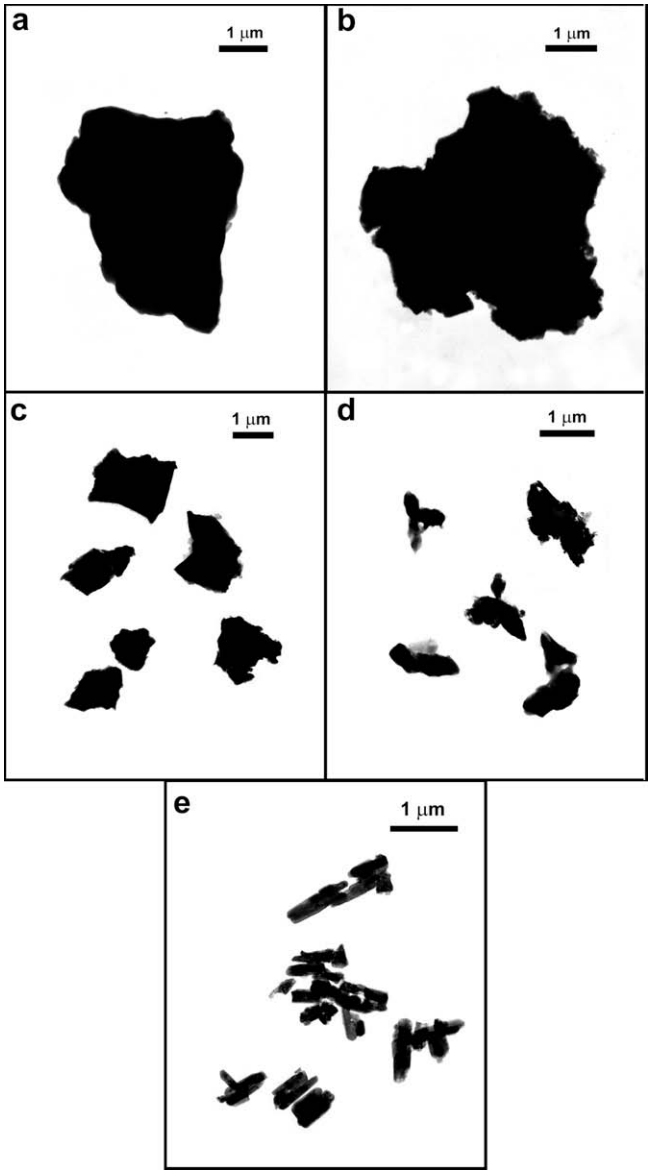

Fig. 7. TEM micrographs of ultrasonicated BC and PC, and MCC samples: (a) BC-0; (b) PC-0; (c) BC-30; (d) PC-30; (e) MCC. Horizontal scale bar is 1 μm.

is desired since there is always a demand for precision engineered cellulosic materials to incorporate in bio-nanocomposites.

References

Baxter, S., Zivanovic, S., & Weiss, J. (2005). Molecular weight and degree of acetylation of high-intensity ultrasonicated chitosan. *Food Hydrocolloids, 19*(5), 821–830.

Cao, Y., & Tan, H. (2004). Structural characterization of cellulose with enzymatic treatment. *Journal of Molecular Structure, 705*(1–3), 189–193.

Carrillo, F., Colom, X., Suñol, J. J., & Saurina, J. (2004). Structural FTIR analysis and thermal characterisation of lyocell and viscose-type fibres. *European Polymer Journal, 40*(9), 2229–2234.

Chen, R. H., Chang, J. R., & Shyur, J. S. (1997). Effects of ultrasonic conditions and storage in acidic solutions on changes in molecular weight and polydispersity of treated chitosan. *Carbohydrate Research, 299*(4), 287–294.

Cote, G. L., & Willet, J. L. (1999). Thermomechanical depolymerization of dextran. *Carbohydrate Polymers, 39*(2), 119–126.

Dupont, A.-L. (2003). Cellulose in lithium chloride/*N*,*N*-dimethylacetamide, optimisation of a dissolution method using paper substrates and stability of the solutions. *Polymer, 44*(15), 4117–4126.

El-Sakhawy, M., & Hassan, M. L. (2007). Physical and mechanical properties of microcrystalline cellulose prepared from agricultural residues. *Carbohydrate Polymers, 67*(1), 1–10.

Gronroos, A., Pirkonen, P., & Ruppert, O. (2004). Ultrasonic depolymerization of aqueous carboxymethylcellulose. *Ultrasonics Sonochemistry, 11*(1), 9–12.

Kamide, K., & Nishiyama, K. (2001). Cuprammonium processes. In C. Woodings (Ed.), *Regenerated cellulose fibres* (pp. 88–155). Cambridge: Woodhead Publishing in conjunction with the Textile Institute.

Kim, U. J., Kuga, S., Wada, M., Okano, T., & Kondo, T. (2000). Periodate oxidation of crystalline cellulose. *Biomacromolecules, 1*(3), 488–492.

Klemanleyer, K. M., Gilkes, N. R., Miller, R. C., & Kirk, T. K. (1994). Changes in the molecular-size distribution of insoluble celluloses by the action of recombinant cellulomonas fimi cellulases. *Biochemical Journal, 302*, 463–469.

Klemm, D., Heublein, B., Fink, H.-P., & Bohn, A. (2005). Cellulose: Fascinating biopolymer and sustainable raw material. *Angewandte Chemie International Edition, 44*(22), 3358–3393.

Lii, C.-Y., Chen, C.-H., Yeh, A.-I., & Lai, V. M. F. (1999). Preliminary study on the degradation kinetics of agarose and carrageenans by ultrasound. *Food Hydrocolloids, 13*(6), 477–481.

Liu, H., Bao, J., Du, Y., Zhou, X., & Kennedy, J. F. (2006). Effect of ultrasonic treatment on the biochemphysical properties of chitosan. *Carbohydrate Polymers, 64*(4), 553–559.

Lorimer, J. P., Mason, T. J., Cuthbert, T. C., & Brookfield, E. A. (1995). Effect of ultrasound on the degradation of aqueous native dextran. *Ultrasonics Sonochemistry, 2*(1), S55–S57.

Marx-Figini, M. (1997). Studies on the ultrasonic degradation of cellulose macromolecular properties. *Angewandte Makromolekulare Chemie, 250*(1), 85–92.

Mason, T. J., & Lorimer, J. P. (2002). *Applied sonochemistry: The uses of power ultrasound in chemistry and processing*. Germany: Wiley-VCH Weinheim.

Miyamoto, I., Matsuoka, Y., Matsui, T., Saito, M., & Okajima, K. (1996). Studies on structure of cuprammonium cellulose. 3. Structure of regenerated cellulose treated by cuprammonium solution. *Polymer Journal, 28*(3), 276–281.

Oh, S. Y., Yoo, D. I., Shin, Y., Kim, H. C., Kim, H. Y., Chung, Y. S., et al. (2005). Crystalline structure analysis of cellulose treated with sodium hydroxide and carbon dioxide by means of X-ray diffraction and FTIR spectroscopy. *Carbohydrate Research, 340*(15), 2376–2391.

Portenlanger, G., & Heusinger, H. (1997). The influence of frequency on the mechanical and radical effects for the ultrasonic degradation of dextranes. *Ultrasonics Sonochemistry, 4*(2), 127–130.

Price, G. J., West, P. J., & Smith, P. F. (1994). Control of polymer structure using power ultrasound. *Ultrasonics Sonochemistry, 1*(1), S51–S57.

Roman, M., & Winter, W. T. (2004). Effect of sulfate groups from sulfuric acid hydrolysis on the thermal degradation behavior of bacterial cellulose. *Biomacromolecules, 5*(5), 1671–1677.

Shibazaki, H., Kuga, S., & Okano, T. (1997). Mercerization and acid hydrolysis of bacterial cellulose. *Cellulose, 4*(2), 75–87.

Shibazaki, H., Kuga, S., Onabe, F., & Brown, J. R. M. (1995). Acid hydrolysis behaviour of microbial cellulose II. *Polymer, 36*(26), 4971–4976.

Son, W. K., Youk, J. H., & Park, W. H. (2004). Preparation of ultrafine oxidized cellulose mats via electrospinning. *Biomacromolecules, 5*(1), 197–201.

Striegel, A. M. (2007). Influence of anomeric configuration on mechanochemical degradation of polysaccharides: Cellulose versus amylose. *Biomacromolecules, 8*(12), 3944–3949.

Tayal, A., & Khan, S. A. (2000). Degradation of a water-soluble polymer: Molecular weight changes and chain scission characteristics. *Macromolecules, 33*(26), 9488–9493.

Varma, A. J., & Chavan, V. B. (1995). Thermal properties of oxidized cellulose. *Cellulose, 2*(1), 41–49.

Wang, N., Ding, E., & Cheng, R. (2007). Thermal degradation behaviors of spherical cellulose nanocrystals with sulfate groups. *Polymer, 48*(12), 3486–3493.

Yamamoto, H., Horii, F., & Hirai, A. (2006). Structural studies of bacterial cellulose through the solid-phase nitration and acetylation by CP/MAS ^{13}C NMR spectroscopy. *Cellulose, 13*(3), 327–342.